

Electronic Supporting Information

for

Ferrocene Conjugated Os(II) Complex for Photo-catalytic Cancer Therapy of Triple-negative Breast Cancer Cells

Apurba Mandal,^a Virendra Singh,^b Silda Peters,^c Arif Ali Mandal,^a Tumpa Sadhukhan,^{*c} Biplob Koch,^{*b} Samya Banerjee^{*a}

^aDepartment of Chemistry, Indian Institute of Technology (BHU), Varanasi, Uttar Pradesh 221005, India (Email: samya.chy@itbhu.ac.in)

^bDepartment of Zoology, Institute of Science, Banaras Hindu University, Varanasi, Uttar Pradesh 221005, India (Email: biplob@bhu.ac.in)

^cDepartment of Chemistry, SRM Institute of Science and Technology, Kattankulathur, Tamil Nadu 603203, India (Email: tumpas@srmist.edu.in)

Table of Content	Page No
1. Materials	3
2. Instrumentation	3
3. Methods	
3.1 NMR spectroscopy	3
3.2 UV-Vis. spectroscopy	3-4
3.3 Photo-stability study	4
3.4 Lipophilicity measurement	4
3.5 DFT/TD-DFT calculation	4-5
3.6 Detection of singlet oxygen (¹ O ₂) generation	5
3.7 Photocatalytic oxidation of NADH	5-6
3.8 Cellular assays	6-8
3.8.1 MTT assay	
3.8.2 Intracellular ROS generation using flow cytometry	
3.8.3 JC-1 assay	
3.8.4 Detection of apoptosis by acridine orange/ethidium bromide dual staining	
3.8.5 Apoptosis Study by Hoechst/PI Dual Staining	
3.8.6 Caspase 3/7 assay	
3.8.7 Statistical analysis	
3.9 Synthesis and Characterization of [Os(Fc-tpy)(bpy)Cl]PF ₆ (OsFe)	8-9
Figures	
Figure S1. Synthetic route of OsFe	10
Figure S2. HRMS of OsFe in acetonitrile	10
Figure S3. ¹ H NMR spectra of OsFe in DMSO-d ₆ (500 MHz)	11
Figure S4. Photo-stability of OsFe in PBS-DMSO (9:1 v/v)	11
Figure S5. Photo-stability of OsFe in DMEM-DMSO (9:1 v/v)	12
Figure S6. Octanol-water partition coefficients of OsFe	12
Figure S7. The optimized structure, HOMO, and LUMO of OsFe	13
Figure S8. SOMO plots of the triplet state of OsFe obtained from at ω-B97XD/def2-SVP in DMSO	13-14
Figure S9. The plot of DPBF absorbance peak at 417 nm vs. time interval upon light irradiation in the absence of complex	15
Figure S10. Generation of H ₂ O ₂ by OsFe during NADH photo-oxidation	15
Figure S11. Cell viability plots of OsFe in MDA-MB-231 and HEK293 cells in the dark and light	16
Figure S12 In-cell ROS generation by OsFe	16
Figure S13. Light-triggered apoptotic cell death of MDA-MB-231 cells induced by OsFe probed by Hoechst and PI	17

Figure S14. Quantitative determination of apoptosis induced by Annexin-V/FITC and PI assay.	17
References	18

1. Materials

All reagents and materials were purchased from commercial sources and used without further purification. $(\text{NH}_4)_2[\text{OsCl}_6]$, 2',7'-Dichlorodihydrofluorescein diacetate (DCFH-DA) and β -Nicotinamide adenine dinucleotide, reduced disodium salt (β -NADH) were purchased from Sigma-Aldrich Chemicals. 2,2'-Bipyridine and 2-acetylpyridine were purchased from Avra Synthesis Pvt. Ltd. (India). Ferrocene carboxaldehyde was purchased from TCI (Tokyo Chemical Industry Co. Ltd.) (Japan). DPBF (1,3-diphenylisobenzofuran) was purchased from BLD Pharma. Ethylene glycol, DMSO, Ethanol, Diethyl-ether, KOH, and aq. NH_3 were purchased from SRL (Sisco Research Laboratories Pvt. Ltd.). MDA-MB-231 and HEK-293 cell lines were procured from NCCS Pune India. DMEM and 12 well cell culture plates were purchased from Genetix Pvt. Ltd. T-25 flask, and 96 well plates were obtained from Eppendorf. Trypsin-EDTA and Penicillin-streptomycin were procured from Gibco. PBS (Phosphate Buffer Saline) was prepared in the laboratory.

2. Instrumentation

Agilent Cary 60 UV-Vis. spectrophotometer was used to record the absorption spectra of the **OsFe**. For the HRMS data, maXis impact 282001.00081 was used. AVH D 500AVANCE III HD 500 MHz OneBay NMR (from BRUKER BioSpin INTERNATIONAL AG) Spectrometer was used to record the NMR spectra. EVOS FL Fluorescence microscopy from Life Technologies was used for cell imaging. Beckman Coulter CytoFLEX LX was used for the FACS analysis.

3. Methods

3.1 NMR spectroscopy

^1H spectra were acquired in NMR tubes in DMSO-d_6 , and the data was processed using MestReNova software.

3.2 UV-Vis. spectroscopy

The UV-Vis. spectra of **OsFe** were recorded with a 1 cm path-length quartz cuvette, and the obtained data was processed using Origin 2019b 64 Bits software. The UV-Vis. spectra of **OsFe** were recorded at ambient temperature from 1100 to 200 nm in PBS-DMSO (9:1, v/v).

3.3 Photo-stability study

The photo-stability study was carried out by time-dependent UV-Vis. spectral measurement. The experiment was done in a PBS-DMSO (9:1, v/v) solution at ambient temperature. For the photo-stability experiment, the solution of **OsFe** was kept under visible light (400-700 nm, 10 J cm⁻²) irradiation.

3.4 Lipophilicity measurement

The partition coefficient of **OsFe** was determined through the shake-flask method.¹⁻³ To prepare water-saturated octanol, 4 ml of octanol was mixed with 1 ml of water and left for 24 hours. Similarly, octanol-saturated water was prepared using the same procedure. **OsFe** was then solubilized in 2 ml of saturated octanol by adding a minimal volume of DMSO, and this solution was added to 2 ml of saturated water. The resulting mixture underwent 24 hours of shaking using a mechanical shaker, followed by settling and separation. The concentration of **OsFe** was subsequently assessed through UV-Vis. absorption spectroscopy. The following equation calculated the partition coefficient,

$$\log P_{o/w} = \log([\text{complex}]_{\text{octanol}}/[\text{complex}]_{\text{water}})$$

3.5 DFT calculation

Density Functional Theory (DFT) calculations were performed to elucidate the electronic structure and photophysical properties of **OsFe**. All the calculations were performed with the Gaussian 16 suite of programs employing DFT and time-dependent DFT methods.⁴ The molecular geometry of the ground state (S_0) and lowest triplet state (T_1) was optimized using the ω B97XD functional with the def2-SVP basis set for all atoms employing restricted and unrestricted Kohn-Sham formalism, respectively. The frontier molecular orbitals (FMOs) and excited state properties were evaluated at ω B97XD/def2-TZVP level of theory. Solvent effects were incorporated using the conductor-like polarizable continuum model (CPCM) with dimethyl sulfoxide (DMSO) as the implicit solvent in all calculations.

To assess the likelihood of triplet state population and the occurrence of intersystem crossing (ISC) processes, spin-orbit coupling (SOC) matrix elements were computed for the relevant

excited states at the ground-state optimized geometry. These calculations were performed using the ORCA quantum chemistry package, and SOC values were determined based on **Equation (1)**.

$$\text{SOC}_{nm} = \sqrt{\sum_i |\langle \psi_{S_n} | \hat{H}_{SO} | \psi_{T_{i,m}} \rangle|^2}; \quad i = x, y, z \quad (1)$$

Where \hat{H}_{SO} represents the spin-orbit Hamiltonian, incorporating the effective nuclear charge. Relativistic effects were accounted for using the zeroth-order regular approximation (ZORA), with the SARC-ZORA-TZVP basis set applied to the metal center and ZORA-def2-TZVP for the main group atoms. To enhance computational efficiency, the RIJCOSX approximation was employed, as recommended in the ORCA manual. Additionally, a very tight SCF convergence criterion was enforced to ensure the accuracy of the calculations.

3.6 Detection of singlet oxygen ($^1\text{O}_2$) generation

Light-induced singlet oxygen ($^1\text{O}_2$) production in solution was detected using 1,3-diphenylisobenzofuran (DPBF) as a $^1\text{O}_2$ probe.^{5,6} **OsFe** (5 μM) and DPBF were mixed in PBS-DMSO (9:1, v/v) solution. The reaction mixture was placed in a quartz cuvette, and the absorbance of DPBF was monitored using UV-Vis spectroscopy at ambient temperature after white light irradiation (400–700 nm) for different time intervals.

The $^1\text{O}_2$ generation quantum yield (Φ_Δ) was calculated by monitoring changes in UV-visible absorption spectra maxima of DPBF in the presence of **OsFe** and $[\text{Ru}(\text{bpy})_3]\text{Cl}_2$. For quantum yield determination, $[\text{Ru}(\text{bpy})_3]\text{Cl}_2$ ($\Phi_\Delta = 0.22$) was used as a standard. The UV-visible absorption spectra of **OsFe** and $[\text{Ru}(\text{bpy})_3]\text{Cl}_2$ were taken at a very low concentration. The singlet oxygen quantum yield values (Φ_Δ) were obtained by using the following equation:

$$\Phi_{\Delta X} = \Phi_{\Delta S} \times (S_X/S_S) \times (F_S/F_X)$$

where Φ_Δ represents $^1\text{O}_2$ generation quantum yield; subscripts x and s designate the sample and $[\text{Ru}(\text{bpy})_3]\text{Cl}_2$, respectively; S stands for the slope of plot matching difference value of absorbance against the irradiation time (s); F stands for the absorption correction factor, which is calculated by $F = 1 - 10^{-\text{OD}}$ (OD represents the optical density of the sample and $[\text{Ru}(\text{bpy})_3]\text{Cl}_2$ at 635 nm).

3.7 Photocatalytic oxidation of NADH by OsFe

Reactions between **OsFe** (5 μM) and NADH (175 μM) in PBS-DMSO (9:1, v/v) (pH = 7.4) solution were monitored by UV-Vis. spectroscopy at ambient temperature upon light irradiation (400-700 nm, 10 J cm^{-2}).

The turnover number (TON) and turnover frequency (TOF) of **OsFe** were calculated using the following equations:

$$[\text{NAD}^+] = [\text{Abs}(339 \text{ nm})_{\text{initial}} - \text{Abs}(339 \text{ nm})_{\text{final}}] / \text{Abs}(339 \text{ nm})_{\text{initial}} \times [\text{NADH}]$$

$$\text{Turnover number (TON)} = [\text{NAD}^+] / [\text{Catalyst}]$$

$$\text{Turnover frequency (TOF)} = \text{Turnover number} / \text{time (h)}$$

During the reaction of **OsFe** (5 μM) with NADH (175 μM) in the DMSO-PBS (1:9, v/v) solution at ambient temperature in the dark or after light irradiation for 60 min (Light source: 400-700 nm, 10 J cm^{-2}), H_2O_2 was detected by Quantofix peroxide test sticks. The H_2O_2 generation level in the solution can be co-related to the color change from white to blue (of the test sticks), indicating 0-25 mg/L amount of H_2O_2 .

3.8 Cellular assays

3.8.1 MTT assay

The cytotoxicity test of **OsFe** has been performed using MTT assay against MDA-MB-231 TNBC (triple negative breast cancer) cells and normal HEK-293 (human embryonic kidney) cells.⁷ In brief, 10,000 cells/well were seeded in two different 96-well cell culture plates, one for light exposure and the other one for dark conditions, and incubated overnight for adherence. After incubation, the cells were treated at different concentrations of **OsFe** (1 μM , 5 μM , 10 μM , 25 μM , and 50 μM) and kept for incubation for 6 h. Thereafter, the **OsFe**-containing medium was discarded, and 100 μL PBS (phosphate buffer saline) was added to each well of all treated 96-well plates. One of those plates was exposed to light (400-700 nm, 10 J cm^{-2}) for 10 min, and subsequently, one was kept under dark conditions. After 10 min, PBS was removed from both the plates and a fresh complete medium was added and incubated for another 18 h. Finally, the medium was discarded, and the fresh MTT-containing medium was added to each well. After incubation of 2 h, the MTT-containing medium was removed, and 100 μL DMSO was added into each well and further incubated for 30 minutes. Thereafter, absorbance was recorded with a multi-plate reader at 570 nm.

3.8.2 Intracellular ROS Generation

The assay was performed by seeding 5×10^4 MDA-MB-231 cells/well in two 12-well cell culture plates (one for light exposure, the second one for dark conditions) followed by treatments with **OsFe** at its IC₅₀ value concentration and incubated for 6 h. After that, a fresh PBS was added to each well after discarding the drug-containing medium, and one plate was exposed to light (400-700 nm, 10 J cm⁻², 10 min), another one was kept in dark condition. After light exposure, PBS was removed, and fresh DMEM was added to each plate and incubated for another 18 h. The cells underwent a PBS wash, followed by adding 10 μM DCFH-DA, followed by incubation at 37 °C for 30 minutes. Finally, images were photographed in a fluorescent microscope under green channels and phase contrast at 100X magnification.

3.8.3 JC-1 assay

Approximately 5×10^4 MDA-MB-231 cells/well in two 12-well cell culture plates (one for light exposure, the second one for dark conditions) were seeded and treated with **OsFe** at IC₅₀ value concentration and allowed to incubate in the dark at 37°C for 6 h. The cells were subjected to a PBS buffer wash after this incubation period. After that, one group of cells was exposed to light (400-700 nm, 10 J cm⁻², 10 min), while the other group remained dark. Cells were then incubated for 18 h in fresh DMEM. Finally, the medium was discarded, and the cells underwent a PBS wash. The cells were then stained using JC-1 dye to visualize changes. Fluorescence-emitting images were captured at 400X magnification (EVOS FL by life technology).

3.8.4 Detection of apoptosis by acridine orange/ethidium bromide dual staining

Acridine orange/ethidium bromide dual staining is generally used in discrimination between live-cell and apoptotic cells.^{8,9} Acridine orange is permissible in all cells, staining nuclei with green emission. Ethidium bromide enters only dead cells with compromised membrane integrity, staining nuclei yellowish-orange.^{8,9} Thus, live cells display normal green nuclei, early apoptotic cells show bright green or yellowish-orange nuclei with condensed or fragmented chromatin, late apoptotic cells display condensed and fragmented orange-red chromatin, and cells undergoing necrosis exhibit structurally intact deep orange nuclei.^{8,9} Briefly, 5×10^4 cells were seeded in 12 well cell culture plates. The cells were then treated with **OsFe** at IC₅₀ concentration and processed using the abovementioned method. The cells were washed with PBS and stained with acridine orange and ethidium bromide at 10 μg mL⁻¹ concentration, followed by 30 min incubation at 37 °C. Finally, the images were taken with an EVOS FL fluorescence microscope (magnification: 400X)

3.8.5 Apoptosis Study by Hoechst/PI Dual Staining

To investigate the nuclear morphology changes after **OsFe** treatments, we performed Hoechst 33342/PI dual staining. For this, 5×10^4 MDA-MB-231 cells/well were seeded in two 12-well plates (one for light exposure, the second one for dark conditions) supplemented with complete DMEM followed by treatments with **OsFe** at the IC₅₀ value concentration and incubated for 6 h. Then, the drug-containing medium was discarded, fresh PBS was added to each well, one plate was exposed to light (400-700 nm, 10 J cm⁻², 10 min), and another one was kept in the dark condition. After light irradiation, PBS was removed, and fresh DMEM was added to each plate and incubated for another 18 h at 37 °C in a humidified 5% CO₂ incubator. Finally, staining with 10 µg/mL PI and 10 µg/mL Hoechst 33342 was done, and images were captured in a fluorescent microscope in phase contrast, red and blue channels at 400X magnification.

3.8.6 Caspase 3/7 assay

For the caspase 3/7 assay, the cells were harvested and seeded in two different 24-well culture plates, treated with the **OsFe** at IC₅₀ concentration, and incubated for 12 hours. After that, the **OsFe**-containing medium was removed from each well. Then PBS was added to each well of both plates; one plate was exposed to light irradiation for 10 min, and another was kept in a dark condition. After 12 h of incubation, the cells were collected and stained with caspase 3/7 and sytox according to the manufacturer protocol (CellEvent™ Caspase-3/7 Green Flow Cytometry Assay Kit by thermoScientific). Finally, the cells were processed for experimentation (BeckMan Coulter, USA).

3.8.7 Statistical analysis

The outcome of the results was expressed as mean ± standard error of the three independent repeated experiments. Sample size, i.e., $n = 3$, was used for respective statistical analysis. The statistical analysis was conducted utilizing SPSS 16.0 (SPSS Chicago, IL, USA) software. Results were compared between the dark control and the rest of the group (Control light, **OsFe**+dark, and **OsFe**+light). The statistical analysis was done by One-way ANOVA followed by Tukey's Post Hoc Test. Values of $p < 0.05$ were considered statistically significant.

3.9 Synthesis and Characterization of [Os(Fc-tpy)(bpy)Cl]PF₆ (**OsFe**)

(NH₄)₂OsCl₆ (0.16 mmol, 0.07 g) and Fc-tpy (0.16 mmol, 0.06 g) in 6 mL of ethylene glycol were refluxed at 120 °C for 2 h under an inert atmosphere of N₂. The resulting dark solution was then cooled to room temperature and then stored at -20 °C overnight. The dark precipitate was filtered

and washed several times with water and diethyl ether. After that, the resulting precipitate is used for the next step.

In the next step, [Os(Fc-tpy)Cl₃] (0.11 mmol, 0.08 g) and 2,2'-bipyridine (0.12 mmol, 0.002 g) were mixed in 6 mL ethylene glycol and refluxed for 6 hours at 180 °C under an inert atmosphere of N₂. The resulting solution was cooled down to room temperature, A saturated, aq. NH₄PF₆ solution was added, and the resulting dark red precipitate was then isolated by filtration, washed with water and diethyl ether, and dried under a vacuum overnight. The crude product was then purified by column chromatography on basic alumina, using acetonitrile as the eluent. Yield: *ca.* 75%. C₃₅H₂₇N₅PClF₆FeOs (MW = 944.1252) expected: C 44.53, H 2.88, N 7.42; observed: C 44.82, H 3.09, N 7.14. **OsFe** exhibited good solubility in CH₃CN, DMF, and DMSO, moderate solubility in EtOH, MeOH, and CHCl₃, and poor solubility in hydrocarbon solvents like pentane, hexane, etc. HRMS in CH₃CN (m/z for [M]⁺): calculated: 800.0919, observed: 800.0913. UV-Vis. in PBS-DMSO (9:1, v/v), where λ_{max} was observed at 530 nm (ε = 7504 M⁻¹cm⁻¹ in PBS-DMSO (9:1, v/v)) and 798 nm (ε = 1441 M⁻¹cm⁻¹ in PBS-DMSO (9:1, v/v)). ¹H NMR (500 MHz, DMSO-d₆): δ/ppm 9.97 (1H), 8.88 (2H), 8.84 (2H), 8.57 (1H), 7.96 (3H), 7.84 (2H), 7.48 (3H), 7.29 (3H), 6.90 (1H), 5.45 (2H), 4.67 (2H), 4.24 (5H).

Figures

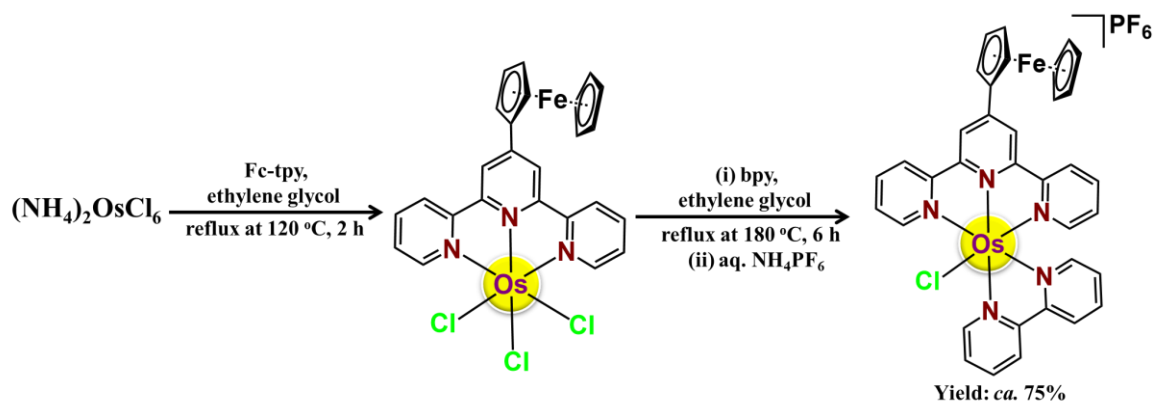


Figure S1. Synthetic scheme of OsFe.

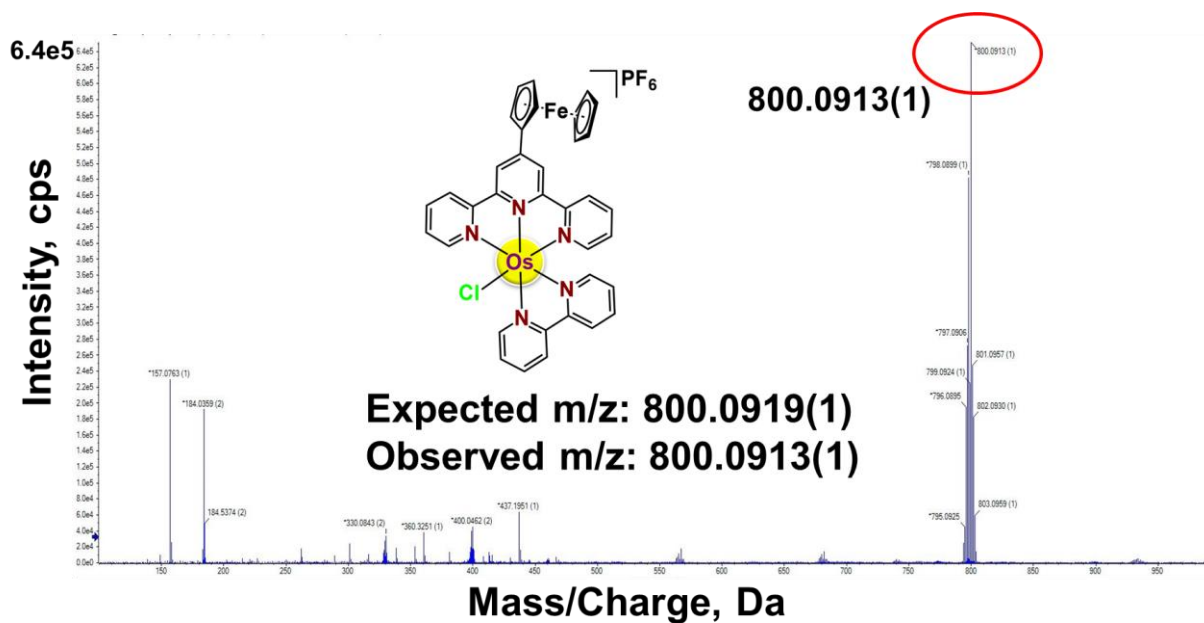


Figure S2. HRMS of OsFe in acetonitrile, showing the corresponding $[\text{M}]^+$ peak.

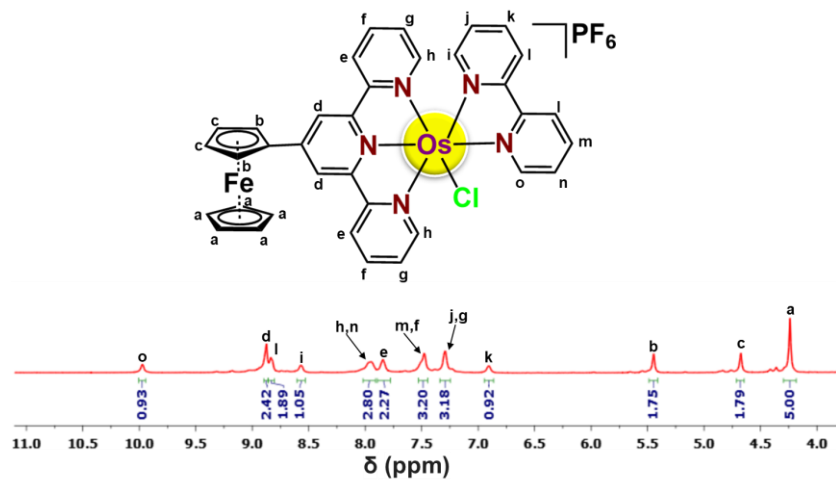


Figure S3. ^1H NMR spectra of OsFe in DMSO- d_6 (500 MHz).

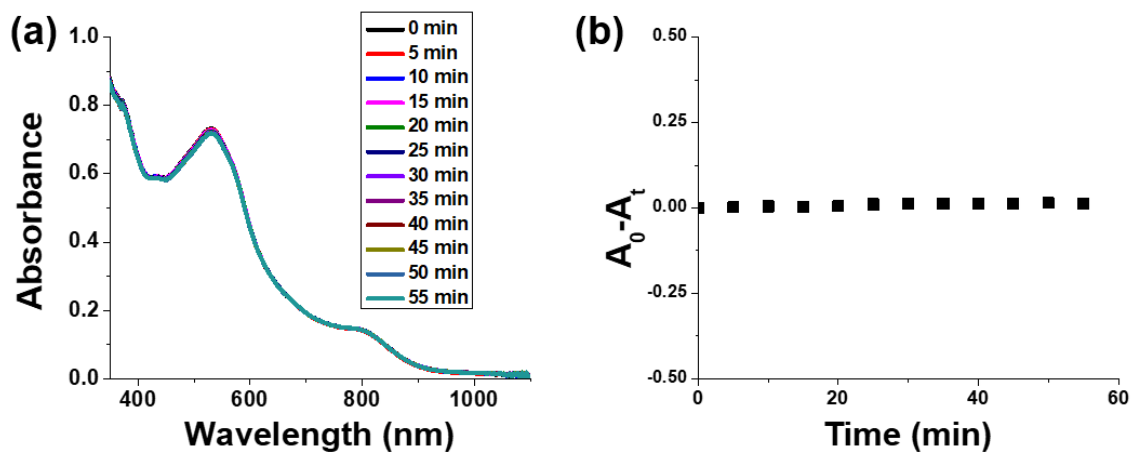


Figure S4. (a) Photo-stability of OsFe in PBS-DMSO (9:1 v/v). (b) Change in absorption (at 530 nm) of OsFe after light irradiation at different times up to 55 minutes.

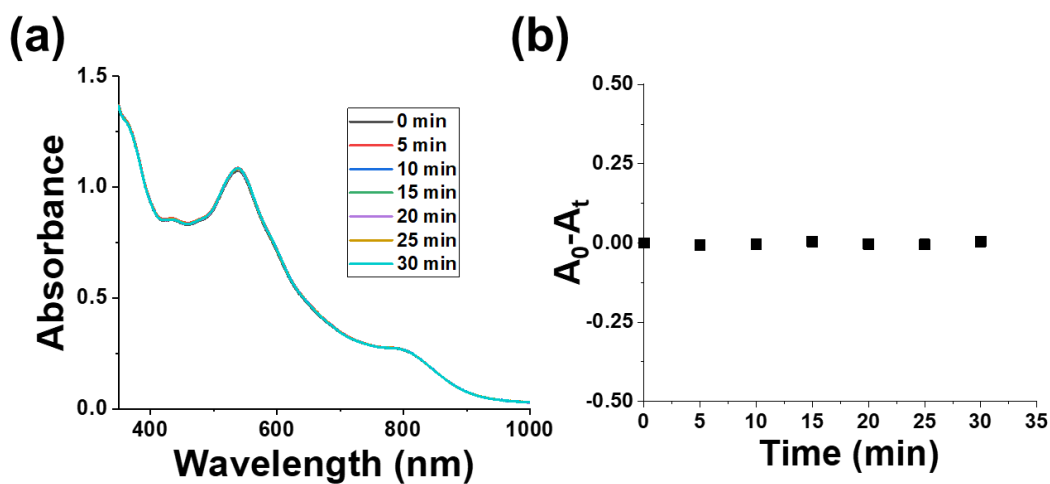


Figure S5. (a) Photo-stability of **OsFe** in DMEM-DMSO (9:1 v/v). (b) Change in absorption of **OsFe** after light irradiation at different times up to 30 minutes.

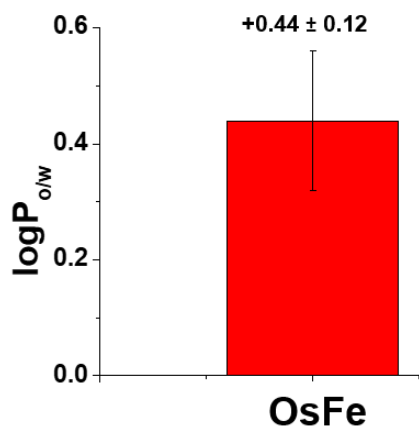


Figure S6. The octanol-water partition coefficient of **OsFe**.

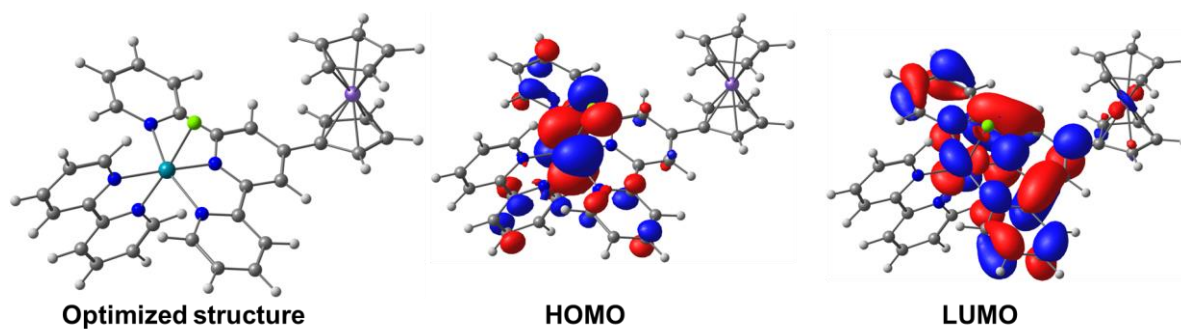


Figure S7. The optimized structure, HOMO, and LUMO of OsFe.

	NTO _o	NTO _v	
S ₀ →S ₁			97 %
S ₀ →S ₂			47.95 %
			37.81 %
			2.36 %

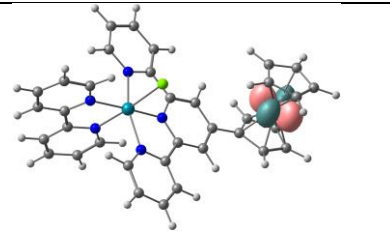
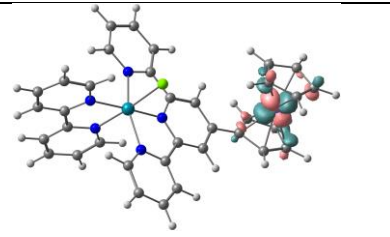
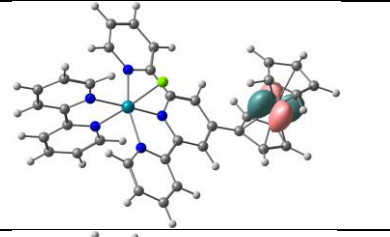
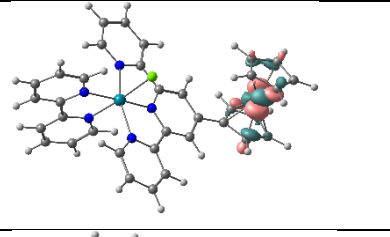
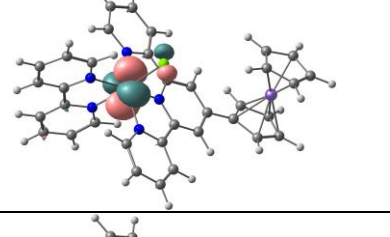
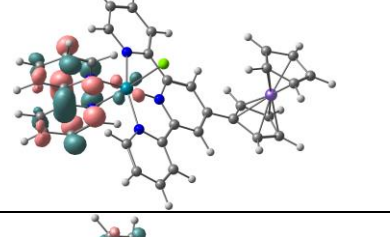
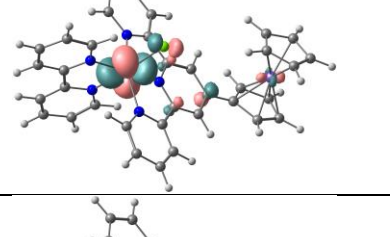
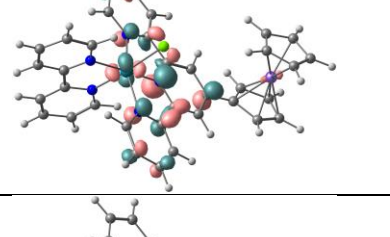
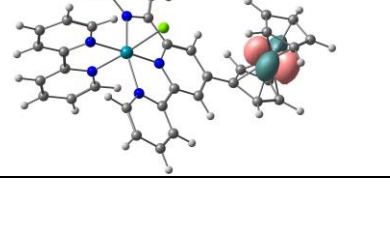
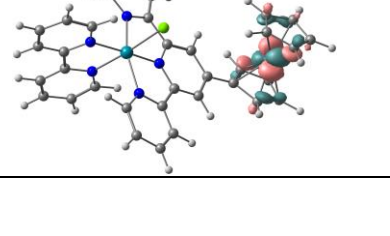
$S_0 \rightarrow S_3$			53.62 %
			36.55 %
$S_0 \rightarrow S_4$			45.11 %
			44.11 %
			2.54 %

Figure S8. Natural Transition Orbitals (NTOs) for the transition of **OsFe** computed at the S_0 geometry. Natural Transition Orbitals occupied (NTO_o), and virtual (NTO_v) involved are represented along with the % contribution.

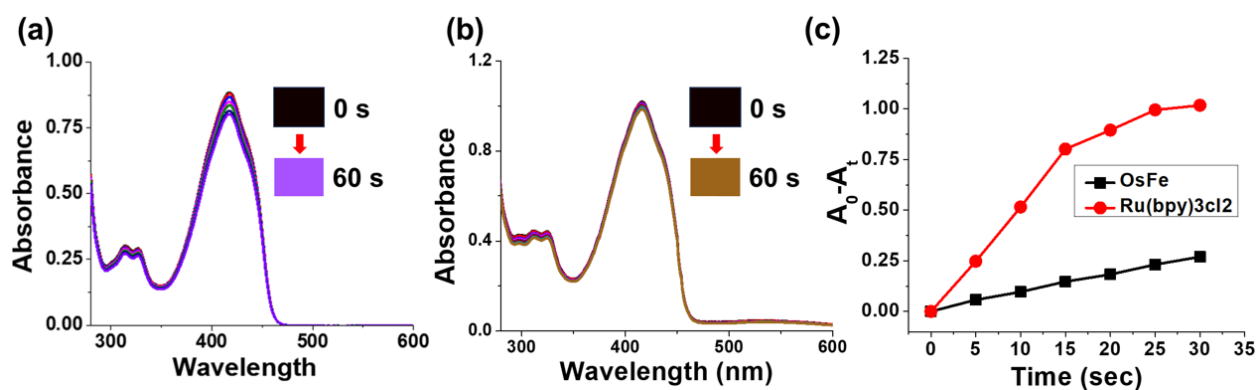


Figure S9. Absorption spectral plots showing the changes in the absorption band of (a) only DPBF under light exposure (Light source: 400-700 nm, 10 J cm^{-2}) and (b) **OsFe**+DPBF under dark. (c) The plot of DPBF absorbance peak at 417 nm vs time interval for [Ru(bpy)₃]Cl₂ and **OsFe** upon light irradiation (10 J cm^{-2} , 400-700 nm).

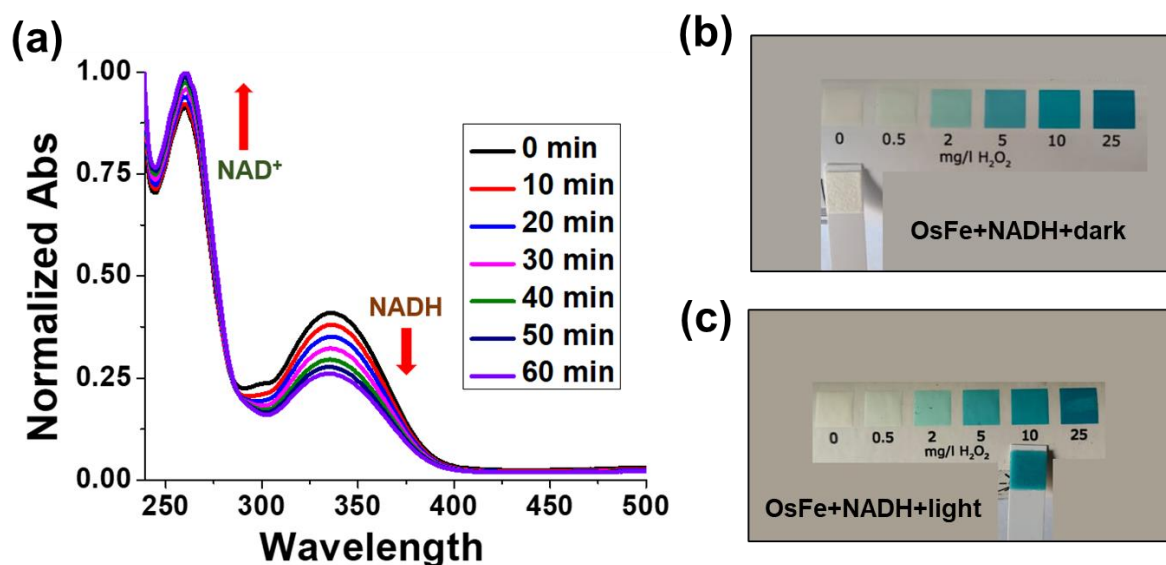


Figure S10. (a) The photocatalytic oxidation of NADH by **OsFe**. Detection of H₂O₂ generation by **OsFe** during NADH oxidation under (b) dark and (c) light (10 J cm^{-2} , 400-700 nm) in PBS-DMSO (9:1 v/v).

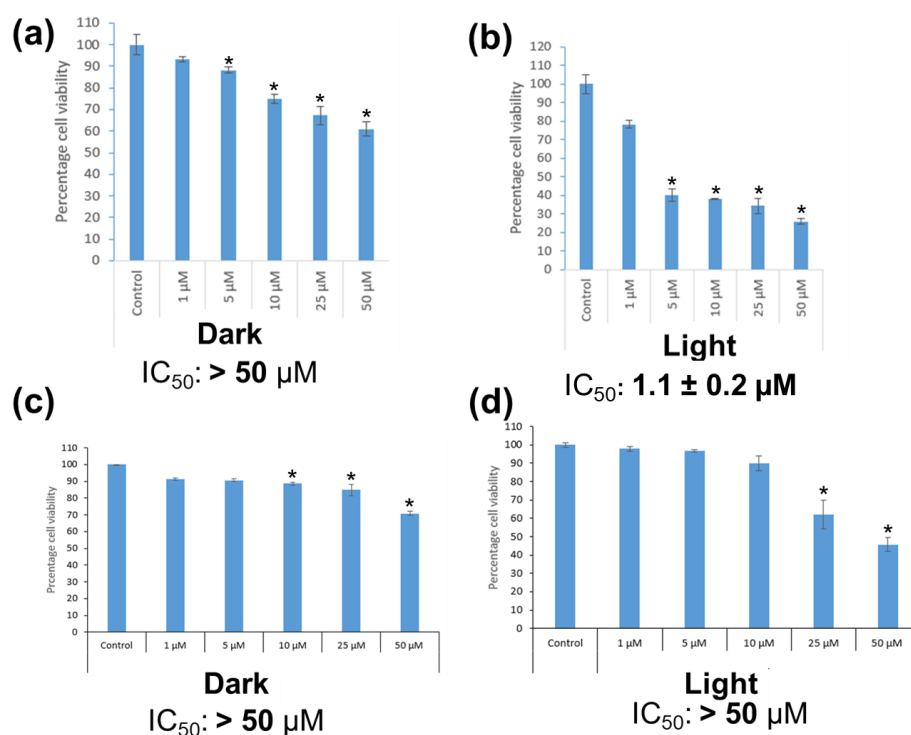


Figure S11. MTT assay-based cell viability plots of **OsFe** in MDA-MB-231 cells (a) under dark, (b) upon light exposure (10 J cm^{-2} , 400–700 nm), and in HEK-293 cells (c) under dark, and (d) upon light exposure (10 J cm^{-2} , 400–700 nm). The statistical analysis done by One-way ANOVA followed the Tuckey test where * denotes $p < 0.05$.

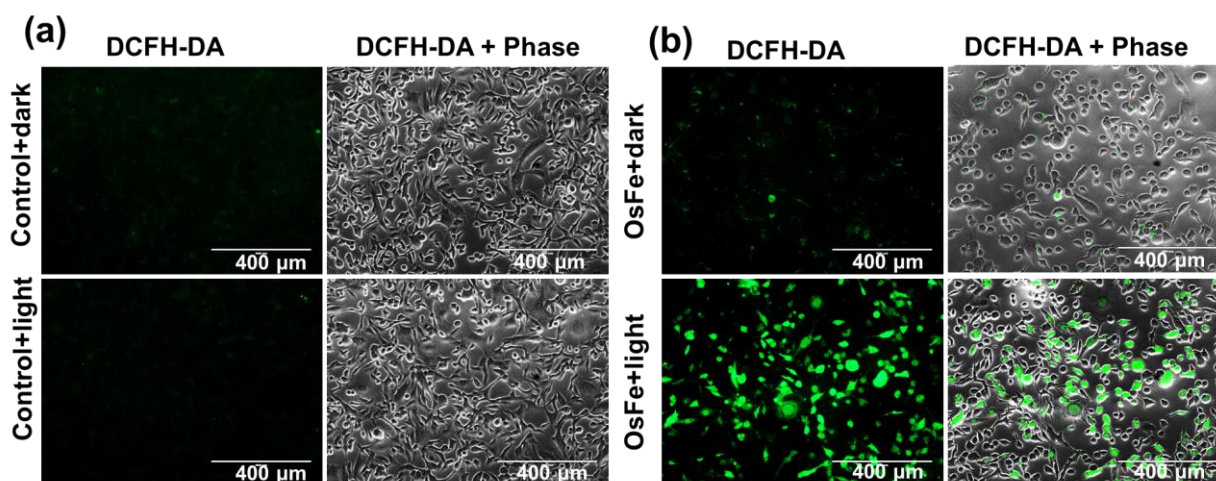


Figure S12. (a) Control experiments for in-cell ROS generation under both dark and light in the absence of **OsFe**. Scale bar: 400 μm (b) ROS generation in MDA-MB-231 cells by **OsFe** under dark and 10 J cm^{-2} , 400-700 nm light (detected using DCFH-DA probe). Scale bar: 400 μm .

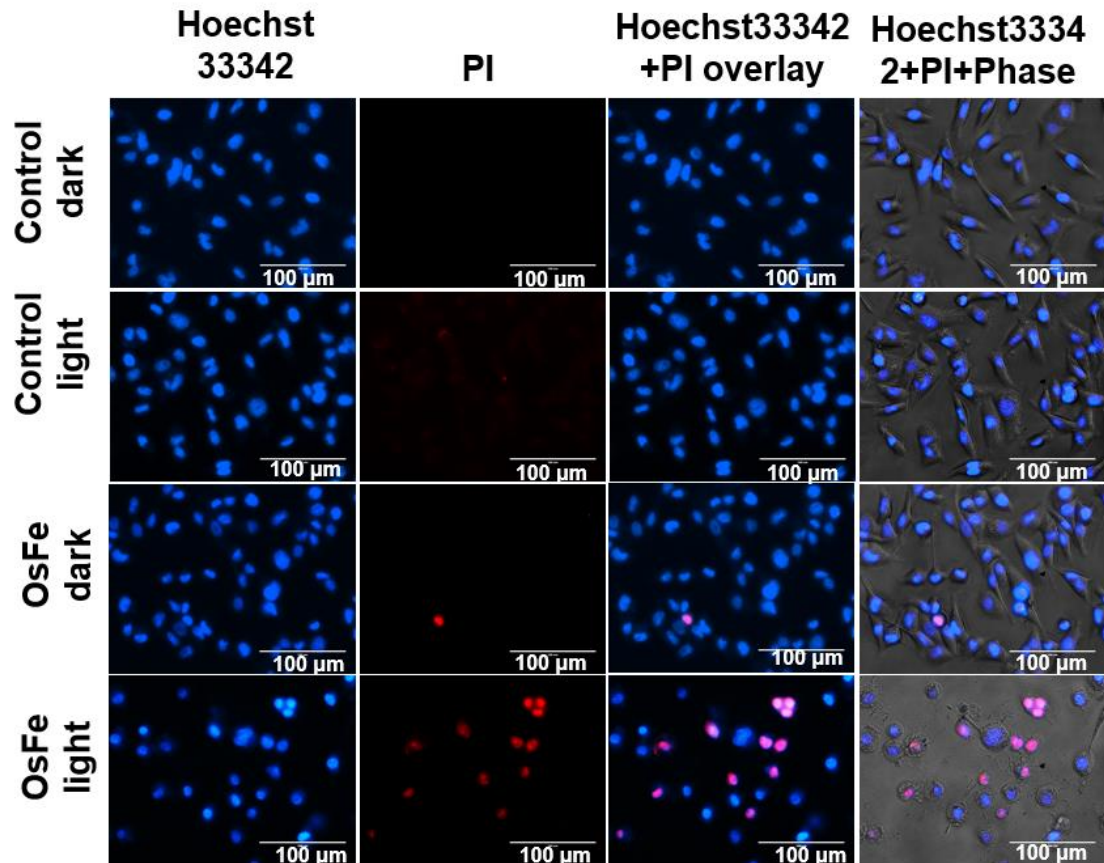


Figure S13. Light-triggered apoptotic cell death of MDA-MB-231 cells induced by OsFe probed by Hoechst and PI. Scale bar: 100 μm .

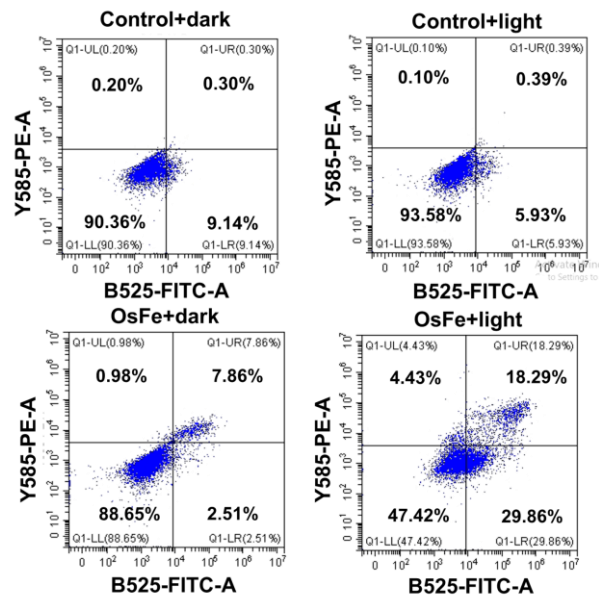


Figure S14. Quantitative determination of apoptosis induced by OsFe by Annexin-V/FITC and PI assay.

References:

1. A. A. Mandal, V. Singh, S. Saha, S. Peters, T. Sadhukhan, R. Kushwaha, A. K. Yadav, A. Mandal, A. Upadhyay, A. Bera, A. Dutta, B. Koch, and S. Banerjee, *Inorg. Chem.*, 2024, **63**, 7493-7503.
2. U. Das, S. Shanavas, A. H. Nagendra, B. Kar, N. Roy, S. Vardhan, S. K. Sahoo, D. Panda, B. Bose and P. Paira, *ACS Appl. Bio Mater.*, 2023, **6**, 410-424.
3. M. Kubanik, H. Holtkamp, T. Söhnel, S. M. F. Jamieson, and C. G. Hartinger, *Organometallics* 2015, **34**, 5658-5668.
4. (a) M. J. Frisch, G. W. Trucks, H. B. Schlegel, G. E. Scuseria, M. A. Robb, J. R. Cheeseman, G. Scalmani, V. Barone, G. A. Petersson, H. Nakatsuji, X. Li, M. Caricato, A. V. Marenich, J. Bloino, B. G. Janesko, R. Gomperts, B. Mennucci, H. P. Hratchian, J. V. Ortiz, A. F. Izmaylov, J. L. Sonnenberg, D. Williams-Young, F. Ding, F. Lipparini, F. Egidi, J. Goings, B. Peng, A. Petrone, T. Henderson, D. Ranasinghe, V. G. Zakrzewski, J. Gao, N. Rega, G. Zheng, W. Liang, M. Hada, M. Ehara, K. Toyota, R. Fukuda, J. Hasegawa, M. Ishida, T. Nakajima, Y. Honda, O. Kitao, H. Nakai, T. Vreven, K. Throssell, J. A. Montgomery Jr., J. E. Peralta, F. Ogliaro, M. J. Bearpark, J. J. Heyd, E. N. Brothers, K. N. Kudin, V. N. Staroverov, T. A. Keith, R. Kobayashi, J. Normand, K. Raghavachari, A. P. Rendell, J. C. Burant, S. S. Iyengar, J. Tomasi, M. Cossi, J. M. Millam, M. Klene, C. Adamo, R. Cammi, J. W. Ochterski, R. L. Martin, K. Morokuma, O. Farkas, J. B. Foresman and D. J. Fox, *Gaussian 16, Revision A.03*, Gaussian, Inc., Wallingford CT, 2016; (b) R. Kushwaha, V. Singh, S. Peters, A. K. Yadav, T. Sadhukhan, B. Koch, and S. Banerjee, *J. Med. Chem.*, 2024, **67**, 6537–6548.
5. A. A. Mandal, A. Upadhyay, A. Mandal, M. Nayak, M. S. K. S. Mukherjee, and S. Banerjee, *ACS Appl. Mater. Interfaces*, 2024, **16**, 28118-28133.
6. T. Entradasa, S. Waldrona, M. Volk, *J. Photochem. Photobiol. B* 2020, **204**, 111787.
7. A. K. Mehata, V. Singh, Vikas, N. Singh, A. Mandal, D. Dash, B. Koch, M. S. Muthu, *ACS Appl. Mater. Interfaces* 2023, **15**, 34343-34359.
8. A. Paul, P. Singh, M. L. Kuznetsov, A. Karmakar, M. F. C. G. D. Silva, B. Koch, and A. J. L. Pombeiro, *Dalton Trans.*, 2021, **50**, 3701-3716.
9. A. Kumar Yadav, V. Singh, S. Acharjee, S. Saha, R. Kushwaha, A. Dutta, B. Koch, and S. Banerjee, *Chem. Eur. J.* 2025, **31**, e202403454.